SOILS AND FOUNDATIONS Vol. 47, No. 5, 857–871, Oct. 2007
Japanese Geotechnical Society

LINEAR AND NONLINEAR VALLEY AMPLIFICATION EFFECTS ON SEISMIC GROUND MOTION

P. N. PSARROPOULOS[i], T. TAZOH[ii], G. GAZETAS[iii] and M. APOSTOLOU[iv]

ABSTRACT

Records and analyses have shown that, apart from *soil stratigraphy*, the *geomorphic conditions* (such as those characterising an alluvial valley) tend to modify the amplitude, the frequency content, the duration, and the spatial variability of seismic ground shaking. As most of the related records and studies to date refer to weak motions (and thereby to linear soil response), the question that has been raised is whether and by how much the unavoidably nonlinear soil behaviour during strong shaking may reduce the unavoidable "*valley amplification*" effects. The paper aims at shedding some light on this important issue by analysing numerically the effects of the sub-surface geomorphic conditions of a valley on its ground surface seismic motion, with emphasis on the influence of *soil nonlinearity*. Two-dimensional linear and equivalent-linear ground response analyses are performed to study an alluvial valley in Japan, the behaviour of which had been monitored during many earthquakes in the early 1980's. Then, using the geometry of this valley as a basis, a parametric investigation is performed on the effects of potential soil nonlinearity arising from the increased intensity of base excitation and/or decreased "*plasticity*" *index** of the clayey soil material. It is shown that strong soil nonlinearity may depress the amplitude of the multiply-reflected and, especially of the horizontally propagating Rayleigh waves, leading to substantially lower valley amplification.

Key words: finite-element method, "plasticity" index, soil amplification, soil dynamics, soil nonlinearity, spatial variability, spectral-element method, valley effects (**IGC**: D7/E8/E13)

INTRODUCTION

The term "*local soil effects*" has been used for many years to describe exclusively the influence of *soil stratigraphy* on the seismic ground motion. Such effects are usually taken into account by the well-known one-dimensional (1-D) analysis, assuming parallel soil layers of infinite extent excited by vertically incident waves. The method prevails mainly in the area of *geotechnical earthquake engineering*, thanks to its simplicity and its wide applicability. Furthermore, most of the seismic provisions of building codes worldwide account for soil effects through single amplification factors applied to the acceleration design spectra, factors that have been derived either by statistical compilation of observations or by 1-D amplification studies.

However, during numerous strong earthquakes in recent years (Spitak, 1988; Loma Prieta, 1989; Northridge, 1994; Kobe, 1995; Athens, 1999) the reported variability of ground shaking or the non-uniform distribution of damage could not be sufficiently explained by simple 1-D analysis. Thorough geophysical and geotechnical surveys, in combination with the utilization of small seismographic arrays and various analytical or numerical simulations, have suggested that the aforementioned discrepancy may be attributed to the existence of subsurface irregularities, like alluvial valleys or sedimentary basins (Aki and Larner, 1970; Aki, 1988 and 1993; Trifunac, 1971; Sánchez-Sesma and Esquivel, 1979; Bard and Bouchon, 1980; Sánchez-Sesma et al., 1988; Graves, 1996; Bao et al., 1996; Bard, 1997; Faccioli et al., 1997; Kokusho and Matsumoto, 1998; Bielak et al., 1999, Paolucci, 1999). It was realized that, apart from the soil-material conditions, the geomorphic features of a valley (in 2 dimensions) or a basin (in 3 dimensions) tend to alter and usually aggravate the amplitude, frequency content, duration, and spatial variability of ground shaking.

The main phenomena that constitute the "*valley amplification*" effects on site response have been summarised for the geotechnical community by Aki (1988) and Finn (1991); some newer major seismic events have dramatically reinforced their main conclusions. A typical

* the term "*plasticity*" is in quotation marks because, as it has been experimentally shown, the higher this index, the more *elastic* (rather than *plastic*) cyclic behaviour becomes.

[i] Lecturer, Hellenic Air-Force Academy, Athens, Greece (prod@central.ntua.gr).
[ii] Director, Center for Engineered Solutions, Institute of Technology, Shimizu Corporation, Tokyo, Japan.
[iii] Professor, National Technical University, Athens, Greece.
[iv] Doctoral Candidate, National Technical University, Athens, Greece.
The manuscript for this paper was received for review on June 21, 2006; approved on May 29, 2007.
Written discussions on this paper should be submitted before May 1, 2008 to the Japanese Geotechnical Society, 4-38-2, Sengoku, Bunkyo-ku, Tokyo 112-0011, Japan. Upon request the closing date may be extended one month.

example of *valley effects* is the damage distribution observed during the 1988 Armenia earthquake. Yegian et al. (1994), trying to correlate the observed damage with the ground shaking in the city of Kirovakan, located about 10 to 15 km from the surface outbreak of the fault, pointed out that 1-D analyses substantially underestimated the ground surface motion in a region of Kirovakan in which the soil profile constitutes a small triangular-shaped alluvial valley; the observed damage was adequately explained by Bielak et al. (1999) who provided a satisfactory explanation performing two-dimensional (2-D) ground response analyses for the same valley. Numerical studies have also shown that the extent of damage reported in the Marina District, San Francisco, during the 1989 Loma Prieta earthquake, could be mainly attributed to the 2-D *site* conditions (Bardet et al., 1992; Graves, 1993; Zhang and Papageorgiou, 1996). Graves (1998), simulating the seismic response of the San Fernando basin in the 1994 Northridge earthquake, showed that the subsurface irregularities may have caused a large amplification, especially in the long period ground motions. Finally, during the 1995 Hyogoken-Nambu earthquake, most of the damage in the city of Kobe occurred within the so-called "disaster belt", a narrow zone 1 km wide, nearly 20 km long, located between about 1 to 1.5 kilometers from the Rokko mountain rock outcrop. Numerical analyses by various researchers (Kawase, 1996; Takemiya, 1996; Kokusho and Matsumoto, 1998; Pitarka et al., 1998; Matsushima and Kawase, 1998; Hisada et al., 1998) have supported the idea that the 2-D valley geometry (in combination with the unquestionable forward-rupture directivity effects) had led to that particular concentration of damage.

The above phenomena have been documented either by observations, or multi-dimensional site-specific ground response analyses (in 2 or 3 dimensions). However, most of the available data of the recorded motions refer mainly to weak-motion excitation (small-magnitude earthquakes or microtremors), and most of the analyses are based on the assumption of linearly elastic, or at most, linearly visco-elastic soil behaviour. However, the stress-strain behaviour of soft soils is highly nonlinear. So, it is reasonable to question the range of validity of conclusions drawn on the basis of linear analyses. Almost a decade ago, Aki (1993), referring to the research needs for improving seismic microzonation, pointed out that "*the most urgent requirement is a clear understanding of the nonlinear amplification effect at soil sites*". Despite the seismological and geotechnical evidence of soil nonlinearity only a very small number of published nonlinear analyses have seriously questioned the substantial *aggravation* caused by *weak-motion valley effects*: Marsh et al. (1995), comparing numerically the linear and nonlinear seismic response of simple 2-D alluvial valleys, were the first to demonstrate that soil nonlinearity results in lower peak accelerations and lower response spectra. Zhang and Papageorgiou (1996), simulating the seismic response of the Marina District Basin during the 1989 Loma Prieta Earthquake and utilising an equivalent-linear method (to account for soil nonlinearity), showed that in the case of strong-motion excitation "*three-dimensional (3-D) focusing and lateral interferences, while still present, are not as prominent as in the weak-motion excitation case*". Additionally, the abovementioned study underlined the fact that the energy dissipation during strong-motion excitation dampens substantially the surface waves, and thus, the response of the valley is dominated by the nearly vertically propagating waves. More recently, Sincraian and Oliveira (1998) examined the nonlinear behaviour of Vovli valley in Greece (*see* Raptakis et al., 2000; Chavez-Garcia et al., 2000), while Xu et al. (2002) simulated a hypothetical 3-D basin assuming elastoplastic soil behaviour obeying Drucker-Prager's model. They showed that the amplitude of ground accelerations is significantly reduced due to soil nonlinearity. On the otherhand, Bielak et al. (2000) pointed out that soil nonlinearity during strong-motion excitation reduces the amplitude of *surface waves* only, while the other valley related wave phenomena from the overall local geological structure remain present.

Therefore, a key issue relating to "*valley amplification*" effects, and consequently to microzonation research, is to quantify the degree and extent of the reduction which is effected by soil nonlinearity of the rather huge 2-D or 3-D amplifications often computed, and especially recorded during small-strain excitations, where soil deposits behave linearly.

The present study, trying to shed some light on this important issue, analyses numerically the effects of the subsurface geomorphic conditions of an alluvial valley in Japan on its ground surface seismic motion. The valley, crossed by Ohba Ohashi (bridge), consists of shallow deposits of soft soil surrounded by a relatively-stiff base and quite steep lateral boundaries. As several seismic records have been obtained (at the base and the surface of the valley) during many earthquakes and ambient vibration tests in the past, the examined valley can be considered as a natural experiment (Tazoh et al., 1984, 1988).

The 2-D seismic behaviour of this valley has been examined in the past by various researchers. Ohtsuki et al. (1984), utilising a hybrid method based on the finite-difference and the finite-element methods, calculated the acceleration and displacement waveforms on the ground surface, and the strain distribution over the inclined boundary. The 2-D numerical modelling showed clearly the generation of surface waves from the irregular boundary. Fukuwa et al. (1985) examined the same valley under SH excitation and compared their results with the available records, utilising a hybrid 2-D method combining boundary-element and finite-element methodologies. On the other hand, the insufficiency of 1-D analysis to explain the recorded amplification and the subsequent level of shaking at the ground surface of the valley has been observed by other researchers. For example, Fan (1992) and Gazetas et al. (1993), examining the seismic response of the foundation of the Ohba Ohashi (bridge) performed a 1-D wave propagation analysis. They showed that 1-D theory could not adequately explain the recorded level of

shaking at the ground surface, and concluded that 2-D analysis was necessary to capture the valley effects.

As mentioned above, the "entrapment" of seismic waves in the valley and the generation of surface waves at the edges of the valley are phenomena expected to have the following "*valley amplification*" effects:

- The intensity of the ground shaking may be amplified at certain location more than 1-D wave-theory predicts. We will use the term "*aggravation*" to describe the additional amplification, above the corresponding amplification computed with 1-D analysis. Such aggravation may be observed not only on the amplitude of the ground shaking (in terms of peak ground acceleration or velocity), but on its spectral content as well.
- The spatial variability of the ground surface motion may be substantial, even for closely-spaced locations characterized by the same soil profile. The ensuing differential motions are usually of great interest on the seismic response of long structures such as bridges and pipelines.

The goal of this paper is to capture numerically these effects.

METHODOLOGY OF THIS STUDY

As all the available recorded motions of the Ohba Ohashi site were from weak and relatively weak excitations, linear 2-D ground response analyses were initially conducted, utilising two different numerical models, based on the Finite-Element (FE) method and the so-called Spectral-Element (SE) method, respectively. In both models an incident SV wave excitation was induced.

The linear FE analysis was based on the "*effective seismic excitation*" technique proposed by Bielak and Christiano (1984), and developed by Loukakis (1988). With this approach, the problem of seismic response of a 2-D valley is transformed into an equivalent one, in which the seismic source is located in the interior of the domain of computation. The advantage of this technique is that, by introducing the seismic excitation directly within the region of interest (through equivalent dynamic point forces), the artificial boundary (at the vertical sides and the bottom of the model) is needed exclusively to absorb the scattered energy (radiation damping) of the system. So, the artificial transmitting boundary (dashpots in this case) may be placed as close to the examined region as the accuracy of the absorbing boundary permits; no approximation is involved in the specification of the free field motion. According to the work of Bielak et al. (2003) and Yoshimura et al. (2003), this option permits the discretization of a limited area of the surrounding 'bedrock', minimising thus substantially the size of the model, and consequently the computational cost (in memory and time). The SE modeling was performed by AHNSE (Advanced Hybrid Numerical Solver for Elastodynamics), developed in the framework of the TRISEE Joint European Research Project (Faccioli et al., 1997; Casadei et al., 1997). The excitation is implemented as an incident plane SV wave obtained by imposing the same acceleration to all nodal points belonging to a selected horizontal line, and, as in the FE model, absorbing boundaries were placed around the domain of interest.

The verification of the two numerical models has been performed by successfully reproducing some of the recorded time-histories of the ground surface motion, using as input the recorded ground base motions (Psarropoulos et al., 1999). Additionally, the analyses showed that the spatial variability in ground surface motion was evident for certain excitations even for relatively short distances, despite the identical soil profile of these locations.

Then, to demonstrate the influence of potential nonlinear soil behaviour on the valley amplification of the specific site, nonlinear 2-D ground response analyses were performed, utilising the FE method. Soil nonlinearity was taken into account approximately by an iterative procedure referred to as the *equivalent-linear method*, according to which the values of soil stiffness and damping are consistent with the level of cyclic shear strain. Additionally, "*plasticity*" *index, PI** is known as a decisive factor of modulus degradation curves of clays; higher *PI* results to milder degradation rate at the same effective cyclic shear strain, γ_c (Vucetic and Dobry 1991; Ishibashi and Zhang 1993; Hudson et al., 1994; Ishihara, 1996; Kokusho and Matsumoto, 1998). In our parametric investigation, the nonlinear soil behaviour is provoked either by hypothetically increasing the intensity of the applied excitation or/and by hypothetically decreasing the *PI* of the clayey soil layers. Comparing records and numerical results, it is shown that, when the clayey materials behave linearly (either due to the weakness of excitation or their own high *PI*), the 2-D features of the valley and the relatively sharp impedance contrast with the underlying soil may have a profound effect on the amplitude and the frequency content of the ground surface motion. Additionally, the duration of motion is being prolonged, while spatial variability of certain frequency components is substantial. The development of soil nonlinearity decreases the amplitude of the multiply-reflected and horizontally propagating waves, leading to substantially lower valley amplification effects. Laterally propagating Rayleigh waves and body waves (including their interferences) are particularly sensitive to the relatively-high material damping generated with nonlinear soil re-action. In that case, a better agreement between 1-D and 2-D site response analyses is expected. It is to be mentioned that a limitation of our analysis (and of most published multi-dimensional nonlinear analyses in the literature) is the reliance on the equivalent-linear approximation.

Clearly, this is hardly an ideal way to model soil response for strongly nonlinear behavior in 2 or 3 dimensions. The numerical example and the *state of the art* in

* the term "*plasticity*" is in quotation marks because, as it has been experimentally shown, the higher this index, the more *elastic* (rather than *plastic*) cyclic behaviour becomes.

the reviewed literature make clear that there exists a continued need for more research on nonlinear multi-dimensional analyses and observations.

CHARACTERISTICS OF THE VALLEY AND RECORDED SEISMIC MOTIONS

The valley, the seismic behaviour of which is examined in our study, constitutes a soft alluvial valley near Fujisawa City, Kanagawa prefecture, Japan. As shown in Fig. 1, it is crossed by the Ohba-Ohashi bridge, which is a 600-meters-long road bridge built across Hikichi river. The specific site constitutes a natural experiment, as the valley is characterized by substantial 2-D features, while on the other hand, both valley and bridge have been instrumentally monitored during numerous earthquakes and ambient vibrations in the past (Tazoh et al., 1984, 1988). However, as this study focuses solely on the seismic response of the valley, the seismic motions recorded at the ground base and the ground surfaces are of significant importance. Figure 2 sketches the arrangement of two of the accelerographs (one at the ground base (*GB*) and another at the ground surface (*GS*)), and the simplified geometry of the valley, based on which the numerical models were developed.

The geologic profile consists of a maximum of 20–25 meters of soft Holocene alluvium, underlain by relatively-stiff Pleistocene diluvial deposits of the Sagami Group. The top soil layers consist of extremely soft clayey strata, containing humus and silt. Despite the soil improvement that had been performed before the bridge construction, the standard penetration test values N remained almost zero, while the shear-wave velocity, V_S (measured by down-hole tests) was ranging between 40 to 65 m/s. The underlying substratum consists of layers of stiff clay and sand characterized by N values over 50 and V_S around 400 m/s.

Ground water table is almost at the ground surface, while the water content of the top soil layers exceeds 100 %, reaching at some points 250%, with correspondingly small soil densities. It is important to note that the top soil layers of the valley are characterized by large to extremely high *PI* (in excess of 150), and therefore likely to behave almost linearly even at large strain levels (Vucetic and Dobry, 1991). The main soil-profile characteristics are shown in Fig. 3, while more details can be found in the original publications (Tazoh et al., 1984, 1988).

The earthquake observations had been carried out by the Institute of Technology of Shimizu Corporation (Tazoh et al., 1988). The free-field motion of the valley had been adequately recorded with accelerographs installed almost at the ground surface and at the interface with the underlain relatively-stiff soil that is regarded as the bedrock. From April 1981 to April 1985 fourteen

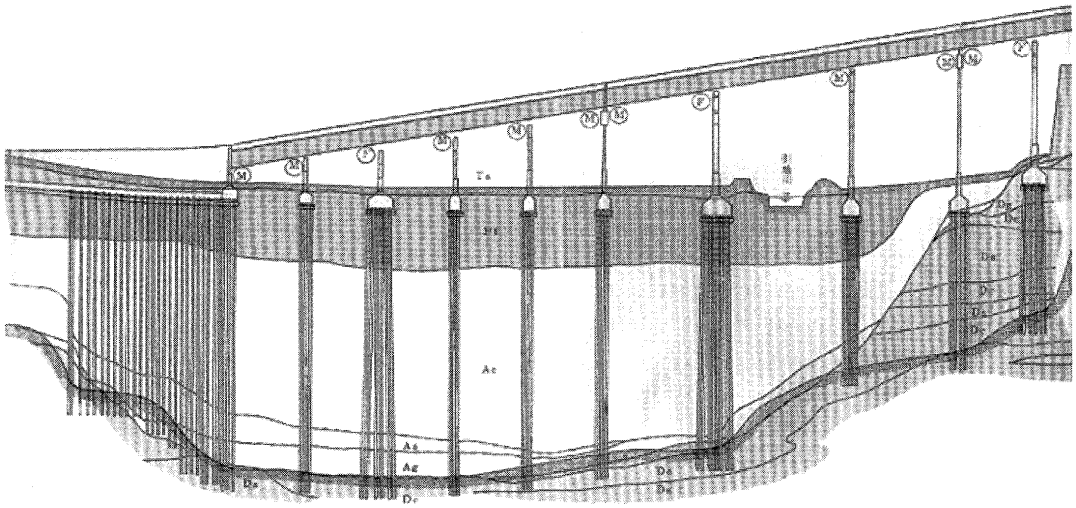

Fig. 1. Cross section of the valley and the Ohba Ohashi (bridge) (Tazoh et al., 1984). Note that the vertical scale is exaggerated; approximate dimensions are given in Fig. 2

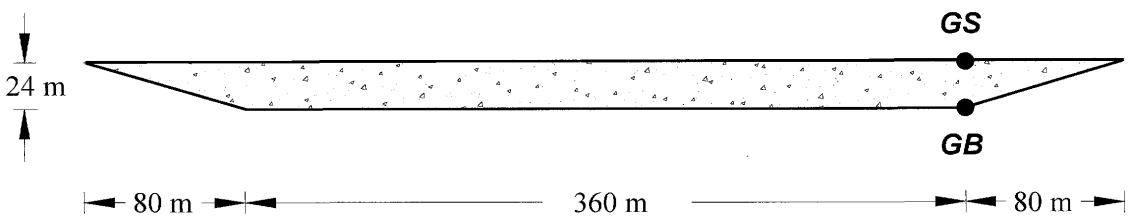

Fig. 2. Simplified geometry of the valley and location of two of the accelerographs, at ground base (*GB*) and ground surface (*GS*)

earthquakes had been recorded in total, and two of them were used in our numerical study (hereafter referred to as Earthquake A and Earthquake B). The latter was the major local earthquake reported for the area during that period (Kanagawa-Yamanashi-Kenzakai earthquake), registering the maximum acceleration levels at the ground surface (0.114 g). The main characteristics of the two seismic events are given in Table 1.

As the in-plane seismic motion (SV wave excitation) is

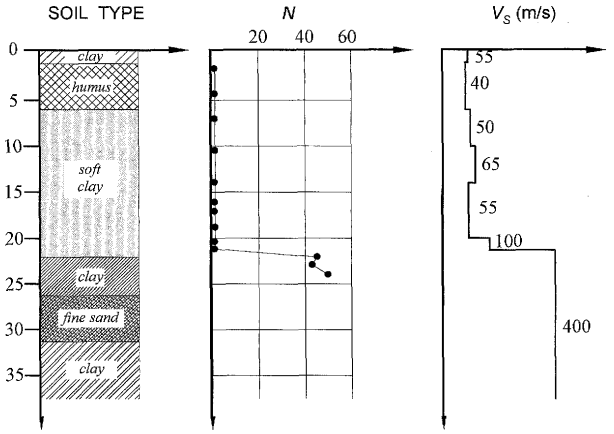

Fig. 3. Typical soil profile of the valley (adopted from Tazoh et al., 1984)

Table 1. Characteristics of the two recorded earthquakes examined (A and B) (from Tazoh et al., 1984)

Earthquake	A	B
Magnitude (JMA)	6	6
Epicentral distance (km)	81	42
Focal depth (km)	70	20
Peak horizontal ground base acceleration* (g)	0.006	0.034
Peak horizontal ground surface acceleration* (g)	0.029	0.114
Peak vertical ground base acceleration (g)	0.005	0.014
Peak vertical ground surface acceleration (g)	0.017	0.029

*in the longitudinal axis H1.

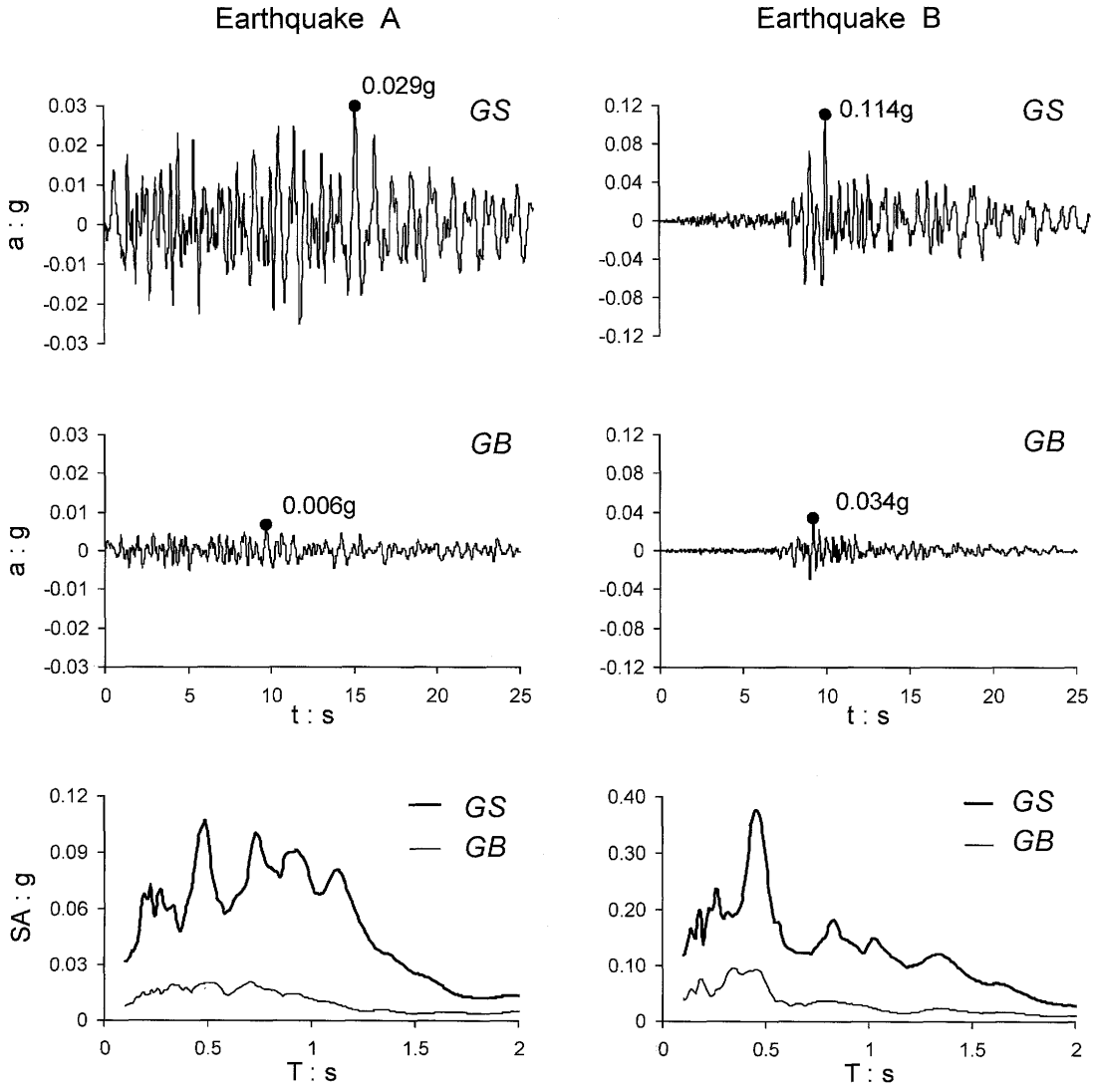

Fig. 4. Acceleration time-histories $\alpha(t)$ and acceleration response spectra $SA(T)$ of the two earthquakes (A and B) recorded at the ground base (*GB*) and the ground surface (*GS*) of the valley, in the longitudinal bridge direction

examined, the recorded acceleration time-histories $\alpha(t)$ in the longitudinal direction (i.e. parallel to the bridge axis) at the ground base of the profile (*GB*) and at the ground surface (*GS*) are given in Fig. 4, along with their response spectra $SA(T)$. It is evident that the peak accelerations are amplified by almost four times, while the spectral amplification seems even higher.

LINEAR SITE RESPONSE ANALYSES

Initially, it was attempted to capture the "*valley amplification*" effects on the ground surface motion of the valley when soil behaves linearly. In that case it is possible to compare directly the numerical results with the available records, as there had been two reasons for the soft soil layer to behave linearly. The first reason was that even the strongest earthquake (Earthquake B) is characterized by low acceleration levels, while the second one was that the soft soil layer is characterized by large *PI*, behaving almost linearly even at large strain levels. To verify both linear models each of the recorded ground base (*GB*) acceleration time histories of the two earthquakes (A and B) was applied as SV wave excitation. The aim was to obtain the recorded acceleration time histories at the ground surface (*GS*).

The geometry and the soil properties of the valley were idealized, assuming a trapezoidal shape and assigning a constant low-strain V_S to the soil stratum equal to 60 m/s (*see* Fig. 5(a)). The figure also shows the four points of interest on the surface (*R1*, *R2*, *R3* and *R4*). Point *R1* is at the middle of the valley surface, while point *R4* is located at the right-hand-side edge of the valley, coinciding with the location of accelerograph *GS*. The FE analyses were performed utilising the commercial code ABAQUS (HKS, 1998), while the SE analyses were performed with the code AHNSE (Faccioli et al., 1997; Casadei et al., 1997).

All the analyses are based on the assumption of linear visco-elastic soil behaviour, which is quite acceptable for earthquakes with relatively-low acceleration levels and for clayey deposits with very high *PI* (as is the case here). By trial-and-error it was discovered that a material damping of the soft soil layer of about 3% (a very reasonable value) led to the most satisfactory results in both recorded earthquakes examined. Note that in both numerical codes (ABAQUS and AHNSE) material damping is of Rayleigh type.

The FE mesh generation (Fig. 5(b)) has been enhanced by the automatic mesh generator NeGe (1992), capable of handling material and geometry irregularities. The mesh

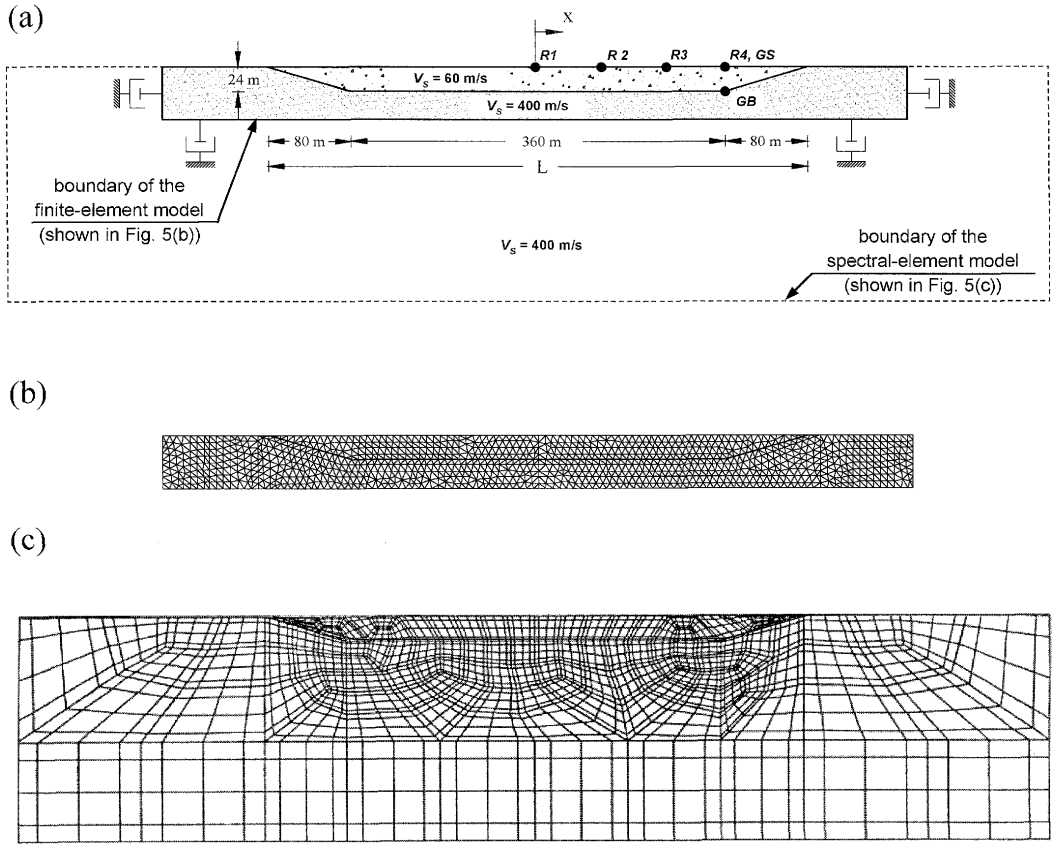

Fig. 5. Numerical models used in the linear analyses: (a) Idealized geometry and shear-wave velocities of the two models (finite-element model, and spectral-element model). In both models special transmitting boundaries minimize spurious wave reflections. Points of interest on the valley surface are designated as *R1*, *R2*, *R3* and *R4*. The location of the ground surface accelerograph (*GS*) coincides with point *R4*. (b) Finite-element discretization of the valley and the surrounding ground. (c) Spectral-element discretization of the valley and the surrounding ground. SV wave excitation is used in both cases. Note that all figures are in the same natural scale (with no exaggerations)

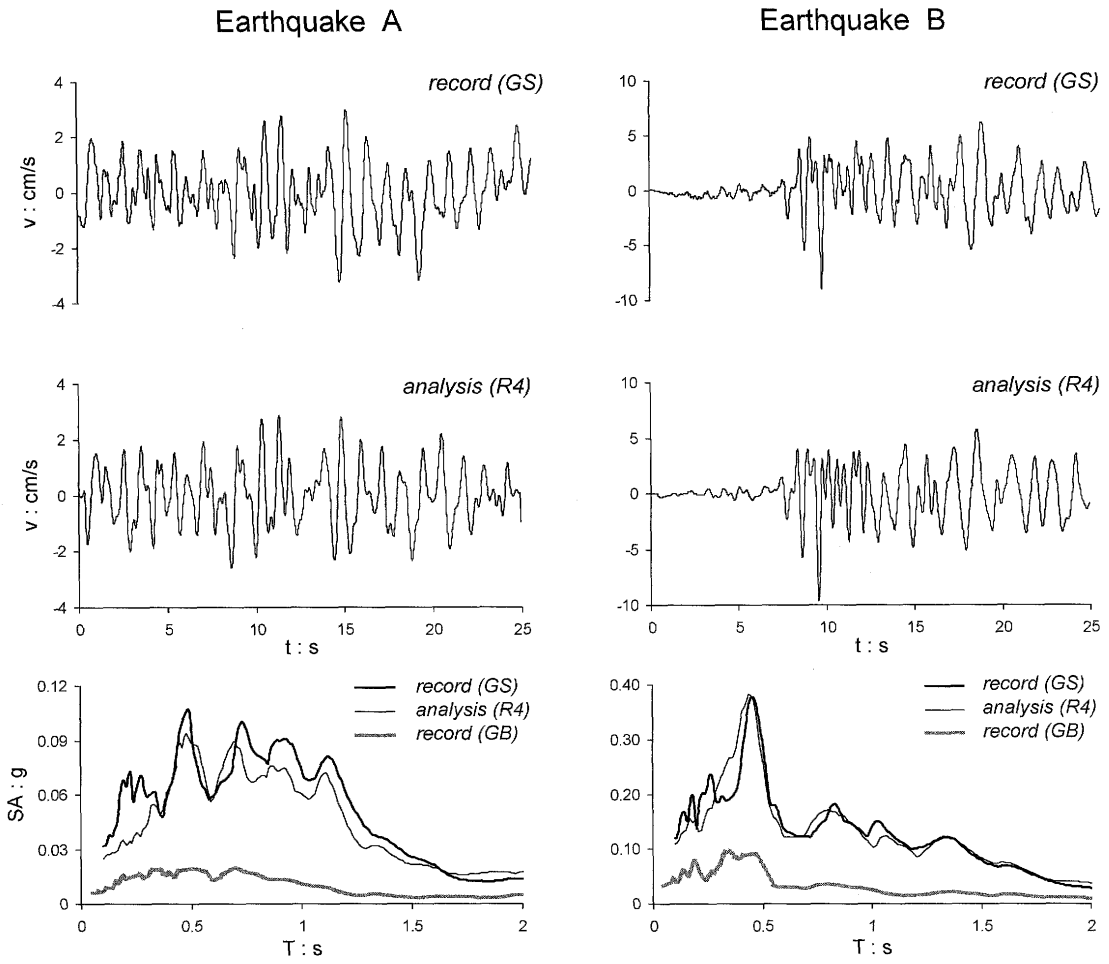

Fig. 6. Comparison (in terms of velocity time histories $v(t)$) between the recorded ground motions (*GB* and *GS*) in the longitudinal direction, and the ground surface motion calculated by the linear finite-element (FE) analyses (*R4*). Acceleration response spectra $SA(T)$ of the two earthquakes are also shown

consists of six-noded triangular elements, the size of which has been tailored to the wavelength of the propagating waves.

On the other hand, the SE analysis was performed by AHNSE. The spectral-element mesh (Fig. 5(c)) consists of *macro* elements, each of which is split into 16 *micro* elements. The size of the elements has also been tailored to the local wavelength of the propagating waves, while the material damping was kept at 3%. The excitation is implemented as an incident plane SV wave obtained by imposing the same acceleration to all nodal points belonging to a selected horizontal line, and, as in the FE model, absorbing boundaries were placed around the domain of interest.

Figure 6 depicts a comparison between the recorded and the FE calculated ground motion for the two seismic events, in terms of velocity, v, and spectral acceleration, *SA*. As there were no additional records (other than *GS*) available on the valley surface, the satisfactory comparison between records and analyses at this location (*GS* versus *R4*) offers a first validation for the linear FE model and the applied method of analysis.

Figures 7 and 8 depict the results obtained for the edge of the valley (*GS*, *R4*) in the case of the strongest event

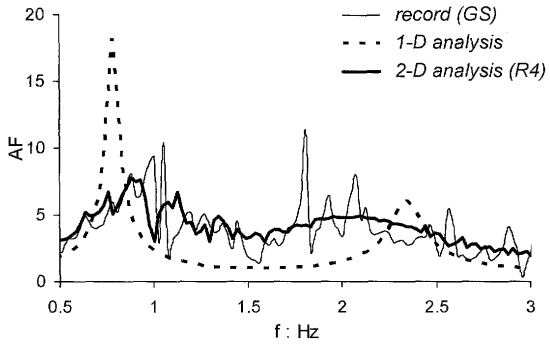

Fig. 7. Earthquake B: Comparison between the *amplification factors* (AF) derived from the: (a) recorded motions, (b) 1-D analysis and (c) 2-D modeling using the FE (and SE)

(Earthquake B). Figure 7 illustrates the amplification factors (AF) predicted by 1-D theory and 2-D numerical analyses, in comparison with the amplification factor derived from the recorded motions. Figure 8 shows the comparison between the recorded and the computed *aggravation factor* (AG), which is defined as the ratio between the amplification factor predicted by the 2-D analysis ($AF_{2\text{-}D}$) and the corresponding predicted by the 1-D

theory ($AF_{1\text{-}D}$). *Aggravation* is of the order of 3 for a wide frequency range, implying thus substantial "*valley amplification*" effects. The inadequacy of 1-D theory to reproduce the recorded motion is evident.

The available records are in accord with the numerical results. The rather small differences in the high-frequency band could be mainly attributed to a variety of factors including the geometry and material uncertainties of the models. Similar are the conclusions drawn by the comparison between the recorded spectral responses at the edge of the valley (*GS*) and the numerical results at point *R4* in Fig. 6, in which the acceleration response spectra computed along the valley surface (for the two earthquakes examined).

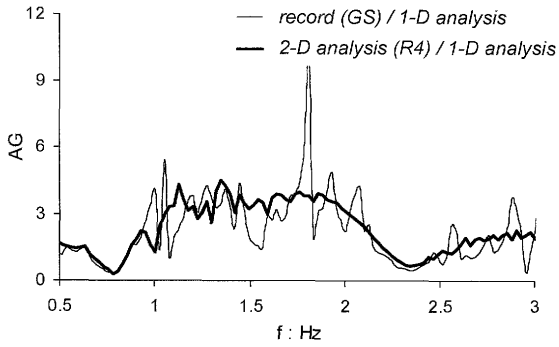

Fig. 8. Earthquake B: Recorded versus computed *aggravation factor* $AG\ (=AF_{2\text{-}D}/AF_{1\text{-}D})$

Additionally, Fig. 9 illustrates the importance of 2-D site response analysis in determining the spatial variability of the ground surface motion. It is interesting to notice that, while approaching the middle of the valley, the response is becoming more intense relatively to the response at the edge, mainly in the case of the high-frequency Earthquake B. This substantial difference in peak spectral accelerations (of the order of 150%) may be attributed to the relatively low values of material damping, increasing thus the constructive interference of the multiply-reflected and horizontally propagating surface Rayleigh and body waves.

NONLINEAR SITE RESPONSE ANALYSES

The previous linear site response analyses were verified by the recorded *aggravation factors*. However, there were suspicions that the rather huge *valley amplification* of the ground motion was merely the outcome of linear soil behaviour, and that the soil nonlinearity could have a profound influence on "*valley amplification*" effects. Although the nonlinear behaviour of soil deposits is strongly depended on the intensity of the excitation, many clayey deposits are characterized by high *PI*, exhibiting nonlinear behaviour only at higher shear-strain

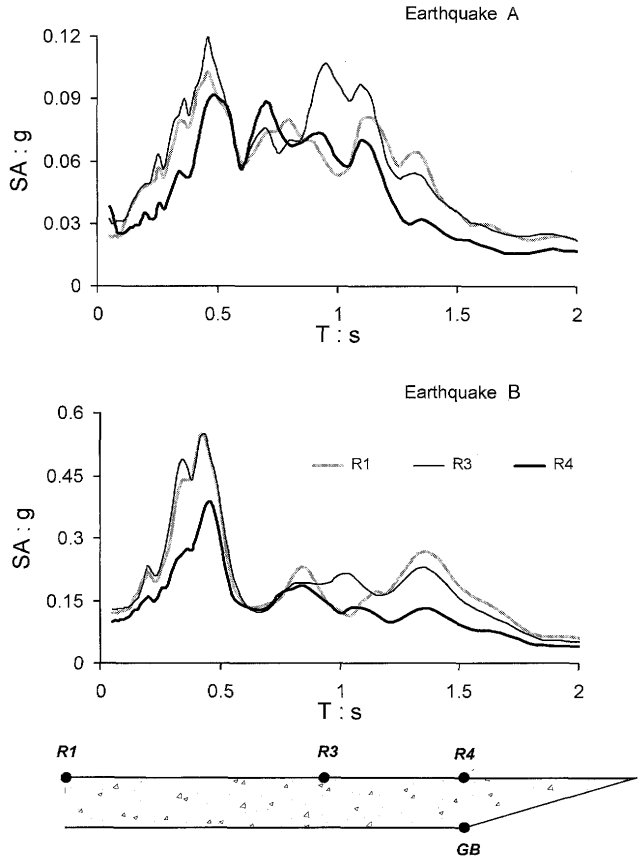

Fig. 9. Acceleration response spectra computed with the FE linear analyses along the surface of the right half of the valley for the two earthquake excitations examined. Only the longitudinal (SV wave induced) motion is studied

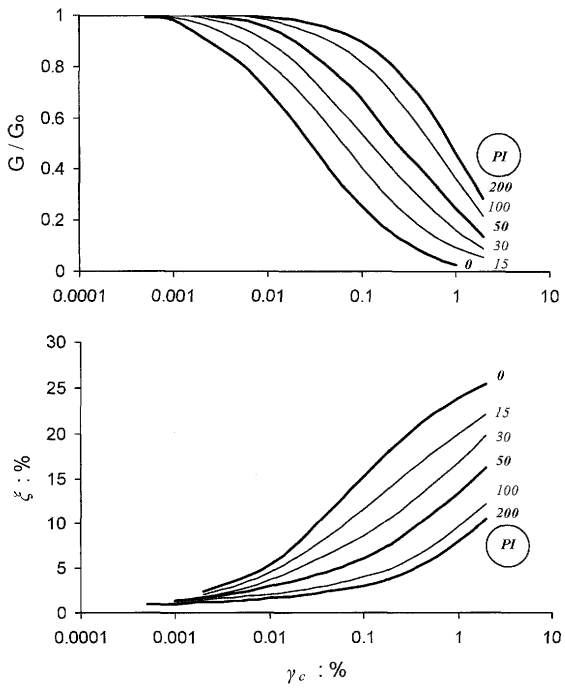

Fig. 10. Dependence of soil shear modulus, *G*, and material damping, ξ, on the "effective" cyclic shear-strain amplitude, γ_c and on the soil "plasticity" index, *PI* (after Vucetic and Dobry, 1991)

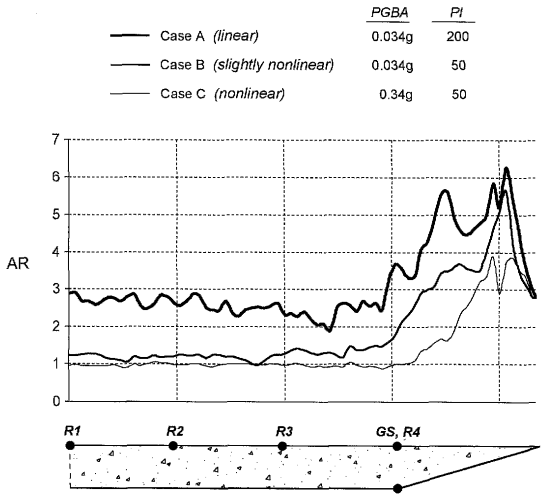

Fig. 11. Equivalent linear analysis for Earthquake B: Distribution along the right half of the valley surface of the *amplification ratio* (*AR*), for two different values of *PGBA* (=0.034 g and 0.34 g), and two different values of plasticity index (*PI*=200 and 50). Notice the progressive reduction of the amplification as the degree of nonlinearity increases (from Case A to Case C)

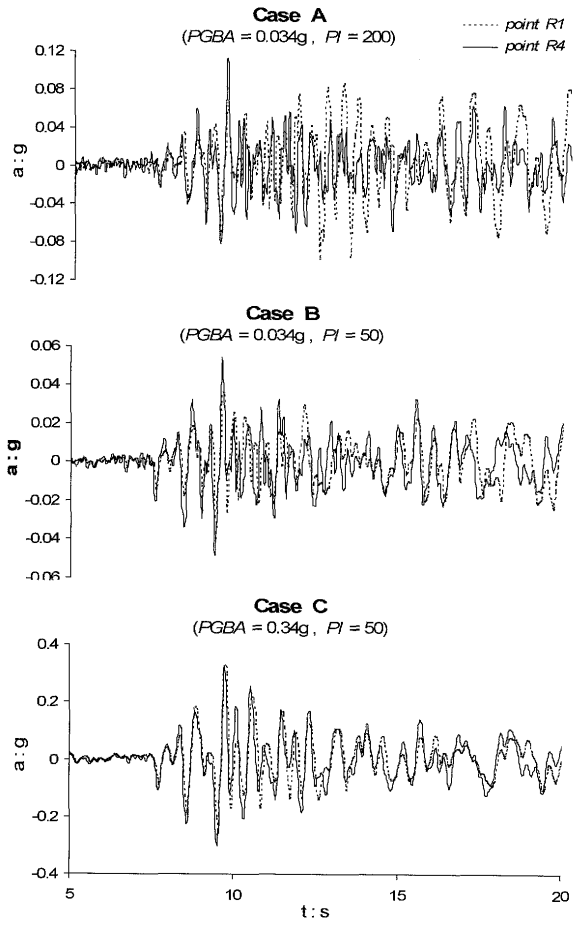

Fig. 12. Equivalent linear analysis for Earthquake B: Acceleration time histories calculated for the middle (*R1*) and the edge (*R4*) of the valley surface for two different values of peak ground base acceleration (*PGBA*=0.034 g and 0.34 g), and three different values of plasticity index (*PI*=200, 50, and 0)

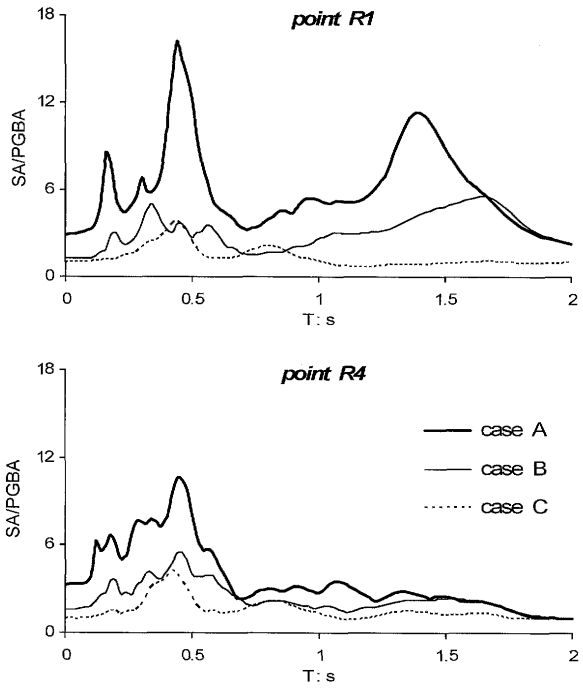

Fig. 13. Equivalent linear analysis for Earthquake B: Acceleration response spectra *SA* (normalized to the peak ground base acceleration *PGBA*) calculated for the middle (*R1*) and the edge (*R4*) of the valley surface. Three cases are examined (case A: linear, case B: slightly nonlinear, and case C: nonlinear)

levels (Kokusho et al., 1982; Vucetic and Dobry, 1991; Ishihara, 1995). A typical example of this behaviour is the Mexico City clay, which during the 1985 earthquake behaved far more linearly than expected, with disastrous consequences for the structures in a central part of the city. This means that, even when the ground shaking of a valley is relatively strong, the aforementioned "*valley amplification*" *effects* may be kept vivid in the case of soft clayey materials.

In this study, to account for a hypothetically nonlinear behaviour of the clayey materials of the examined valley, an extensive investigation was conducted. Two-dimensional equivalent-linear analyses were performed utilising the FE code QUAD4M (Hudson et al., 1994). Soil nonlinearity was taken into account by an iterative procedure according to which the values of soil stiffness and material damping are consistent with a certain percentage ($\approx$65 %) of the maximum shear-strain level. Figure 10 shows the dependence of soil shear modulus, G, and material damping, ξ, on the effective cyclic shear-strain amplitude, γ_c and on the soil "plasticity" index, *PI*. The results of Vucetic and Dobry (1991), shown in Fig. 10, demonstrate that the degree of soil nonlinearity increases with decreasing *PI* (despite the connotation of the term "plasticity"). Note that in this case the confining pressure (i.e. the normal stresses) is related only to the initial shear modulus, G_O. Therefore, increased nonlinearity of a clayey material may be achieved either by increasing the intensity of the excitation, or by reducing the *PI* of the material.

Thus, a parametric study was conducted to examine the influence of (a) the peak ground base acceleration

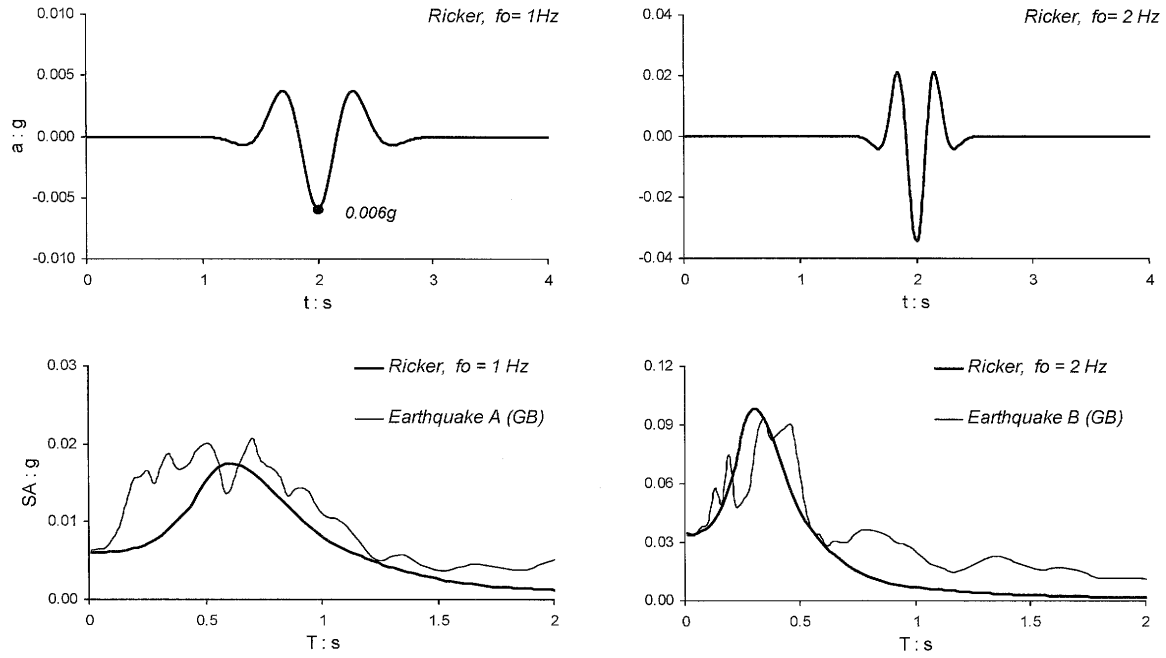

Fig. 14. Acceleration time-histories $a(t)$ and the corresponding acceleration response spectra $SA(T)$ of the two Ricker wavelets used as excitation in our study. The first wavelet, having a characteristic frequency f_o of 1 Hz "covers" a wide period range up to 1.0 s, while the second wavelet (with $f_o = 2$ Hz) covers periods up to 0.5 s. The acceleration response spectra of the two ground base motion (*GB*) of Earthquakes A and B are also included

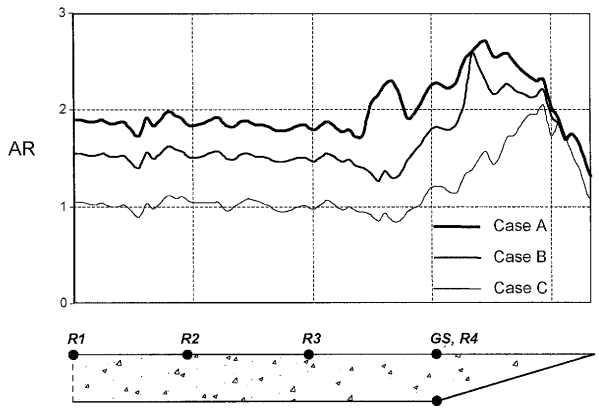

Fig. 15. Equivalent linear analysis for the high-frequency Ricker pulse ($f_o = 2$ Hz): Distribution along the right half of the valley surface of the *Amplification Ratio* (*AR*)

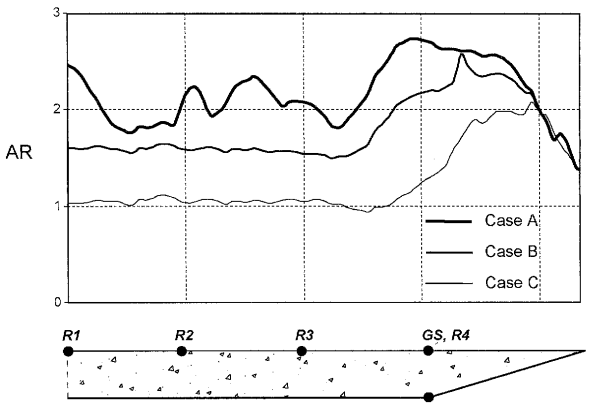

Fig. 16. Equivalent linear analysis for the low-frequency Ricker pulse ($f_o = 1$ Hz): Distribution along the right half of the valley surface of the *Amplification Ratio* (*AR*)

(*PGBA*), and (b) "plasticity" index (*PI*) on the seismic response of the examined valley. Initially, the *PGBA* of Earthquake B is scaled from 0.034 g up to 0.34 g, while *PI* ranges parametrically from 200 to 50. Three cases are thus examined. The first of them coincides with the linear case already examined, while the other two are hypothetical:

- Case A: Linear ($PGBA = 0.034$ g and $PI = 200$)
- Case B: Slightly non-linear ($PGBA = 0.034$ g and $PI = 50$)
- Case C: Non-linear ($PGBA = 0.34$ g and $PI = 50$)

Figure 11 shows for each case the distribution along the valley surface of the *Amplification Ratio* (*AR*), defined as the ratio between the peak ground surface acceleration (*PGSA*) and the peak ground base acceleration (*PGBA*). Comparisons between cases A and B (where the *PGBA* is the same) reveal the influence of *PI* on the seismic response. On the other hand, the comparison between cases B and C shows clearly the influence of the ground shaking intensity. Note that, while moving from case A to case C, *AR* is being substantially reduced, reaching values even lower than unity, implying de-amplification effect.

Similar are the trends of Fig. 12 and 13 for the acceleration time histories and the corresponding acceleration response spectra, respectively, calculated for the middle and the edge of the valley.

The main conclusion is that for a soil deposit with a moderately high "*plasticity*" *index*, increasing the intensity of base excitation reduces the amplification almost

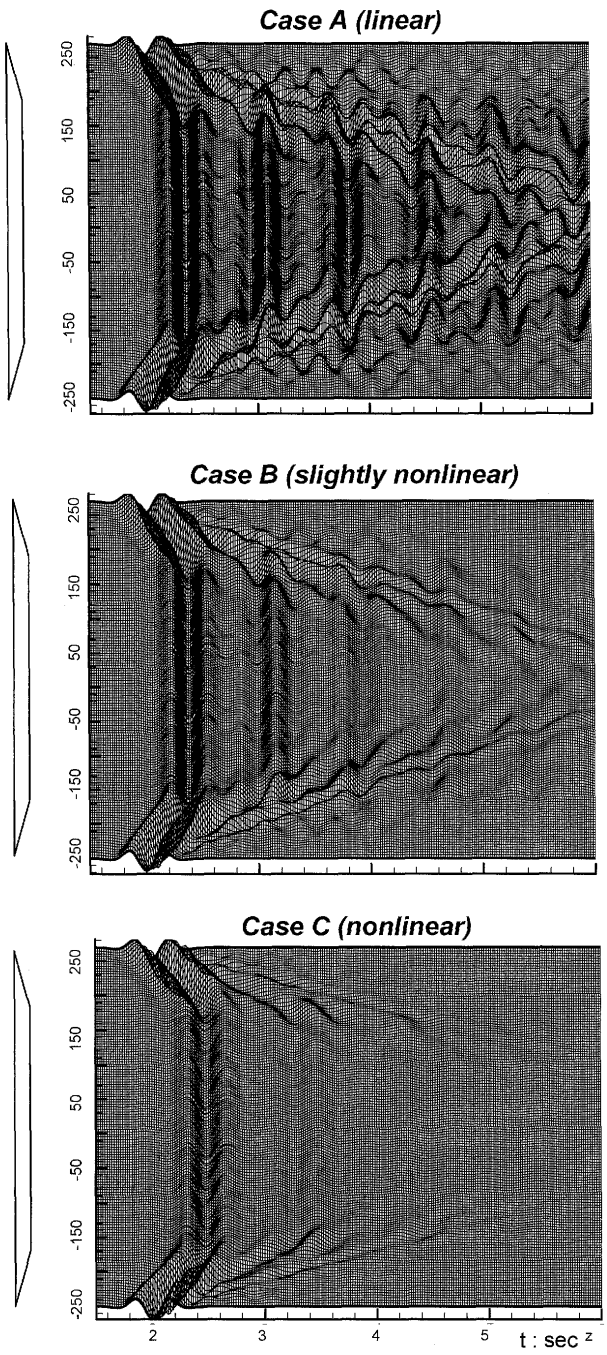

Fig. 17. Wavefields of horizontal acceleration calculated along the surface of the valley for the three cases of nonlinearity examined for the high-frequency Ricker pulse ($f_o = 2$ Hz)

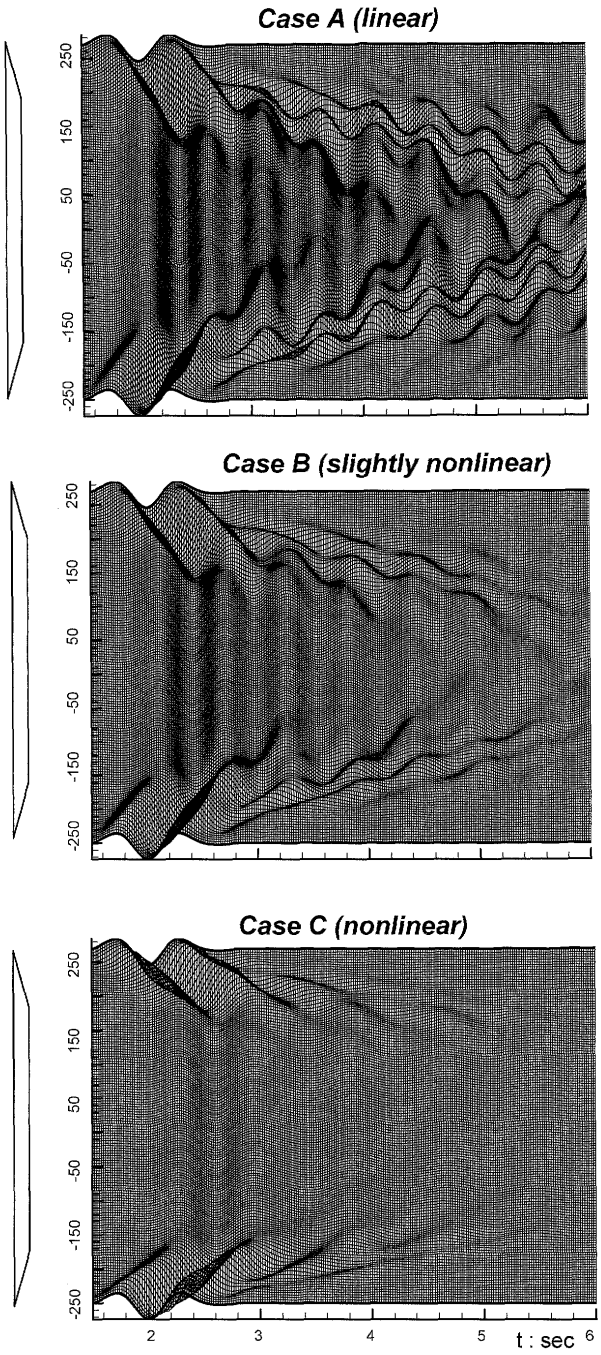

Fig. 18. Wavefields of horizontal acceleration calculated along the surface of the valley for the three cases of nonlinearity examined for the low-frequency Ricker pulse ($f_o = 1$ Hz)

everywhere on the surface. Apparently the increased nonlinearity, with the large hysteretic damping it generates, leads to reduced accelerations of the surface. In addition, waves generated at the edges and propagating laterally across the valley attenuate substantially; thus the undulatory (in space) nature of surface acceleration is diminished. On the other hand, with decreasing *PI* the soil becomes less (*not* more) linear, and the trends are essentially the same as with increasing intensity of motion.

Finally, we notice that the spatial variability of ground shaking may be significant even for relatively short distances. The phenomenon may be of extreme importance for long structures, and could be evaluated with 1-D analysis only in the cases where strongly nonlinear response prevails.

To investigate the influence of soil nonlinearity on the wave field of the valley, the aforementioned parametric study (three cases of soil nonlinearity) was repeated using as base excitation two Ricker pulses of characteristic frequencies $f_o = 1$ Hz and $f_o = 2$ Hz, respectively (Ricker, 1960). Their acceleration time-histories $a(t)$ and the corresponding acceleration response spectra $SA(T)$ are shown in Fig. 14. It is evident that the first Ricker pulse is relatively rich in a wide range of periods, up to 1 sec,

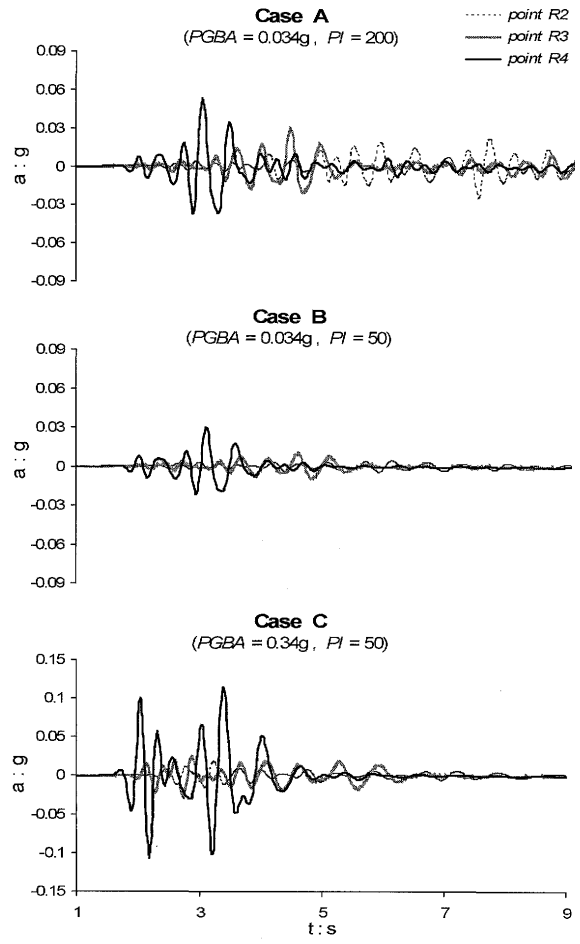

Fig. 19. Time histories of the *parasitic* vertical acceleration calculated along the valley surface in the case of the high-frequency Ricker pulse ($f_o = 2$ Hz)

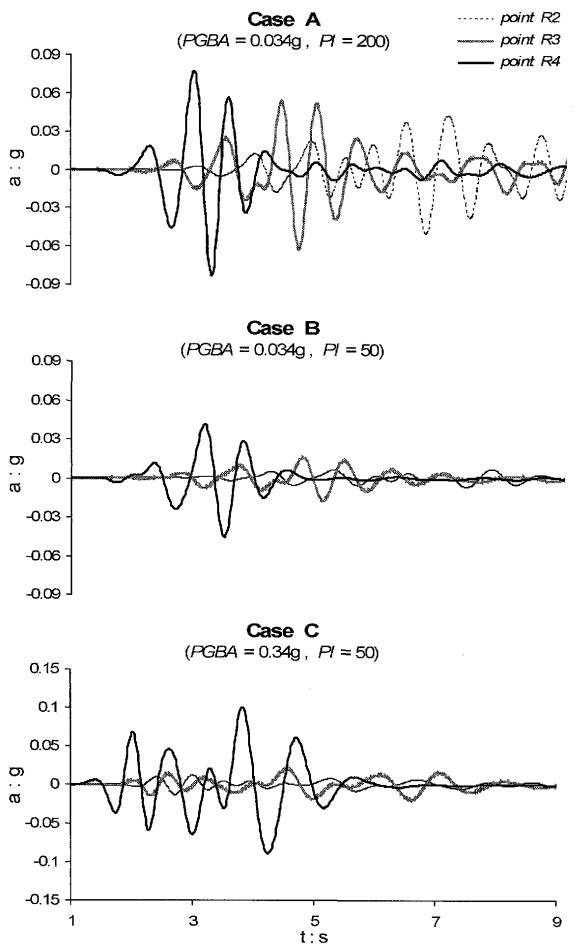

Fig. 20. Time histories of the *parasitic* vertical acceleration calculated along the valley surface in the case of the low-frequency Ricker pulse ($f_o = 1$ Hz)

while the second covers a range of periods up to 0.5 sec. Note that, despite the simplicity of the waveforms, their response spectra are quite similar with the ground base motion of Earthquake A and Earthquake B, respectively.

The distributions along the valley surface of the Amplification Ratio (AR), defined as the ratio between horizontal peak ground surface acceleration and horizontal peak ground base acceleration are given in Figs. 15 and 16.

An illuminating way of visualizing the various types of waves (body and surface), as they propagate in the valley, is the plots of Figs. 17–18 and 23–24. The first two figures plot the horizontal acceleration time histories of numerous closely-spaced points that constitute the ground surface. The resulting shapes reveal various wave phases that can be identified through their respective wave velocities. For instance, in Fig. 17 the seismogram synthetics calculated along the surface of the valley for the four cases of nonlinearity examined in the case of high-frequency Ricker pulse are shown. Especially in the linear case (Case A) the observed waveforms are clearly depicted: (a) vertically propagating incoming SV waves, (b) refracted inclined waves by the wedge-shaped boundary of the valley, and (c) surface Rayleigh waves generated at the edges, and propagating back and forth. The velocity of the surface Rayleigh waves, graphically estimated, is around 120 m/s, while the apparent velocity of the refracted inclined waves is 200 m/s (as theoretically expected).

While shifting progressively from Case A (linear case) to Case C (nonlinear case), both energy dissipation (due to the hysteretic nature of soil behavior) and soil stiffness degradation take place. It is obvious that the energy dissipation dampens all the waveforms. In this way the interferences of vertical or inclined body waves from multiple reflections at the soil-base interface and the free surface are substantially affected, while on the other hand, the laterally propagating surface Rayleigh waves are so strongly attenuated that cannot even be distinguished in the nonlinear case (Case C) at distances beyond the first point from the edge. Nevertheless, the stiffness degradation is responsible for the notable decrease of the Rayleigh wave velocity observed particularly in the slightly nonlinear case.

Similar are the conclusions drawn for the low-frequency case (Ricker pulse of characteristic frequency $f_o =$ 1 Hz), as depicted in Fig. 18.

Finally, it is worth to mention that, despite the

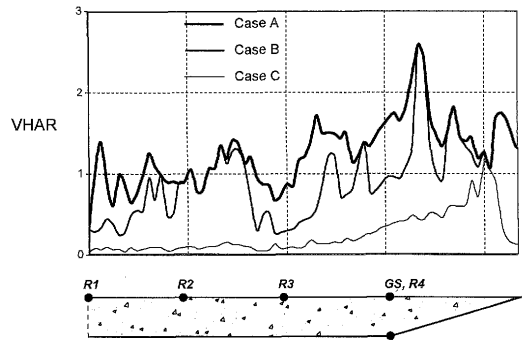

Fig. 21. Equivalent linear analysis for the high-frequency Ricker pulse ($f_0 = 2$ Hz): Distribution along the right half of the valley surface of the *Vertical to Horizontal Amplification Ratio (VHAR)*

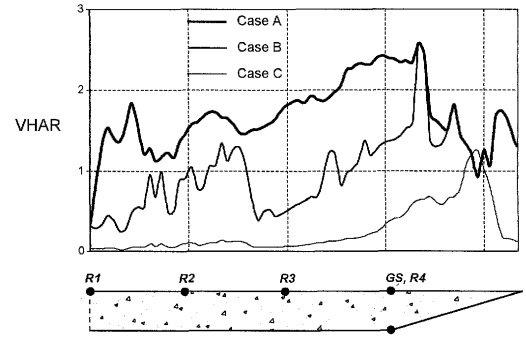

Fig. 22. Equivalent linear analysis for the low-frequency Ricker pulse ($f_0 = 1$ Hz): Distribution along the right half of the valley surface of the *Vertical to Horizontal Amplification Ratio (VHAR)*

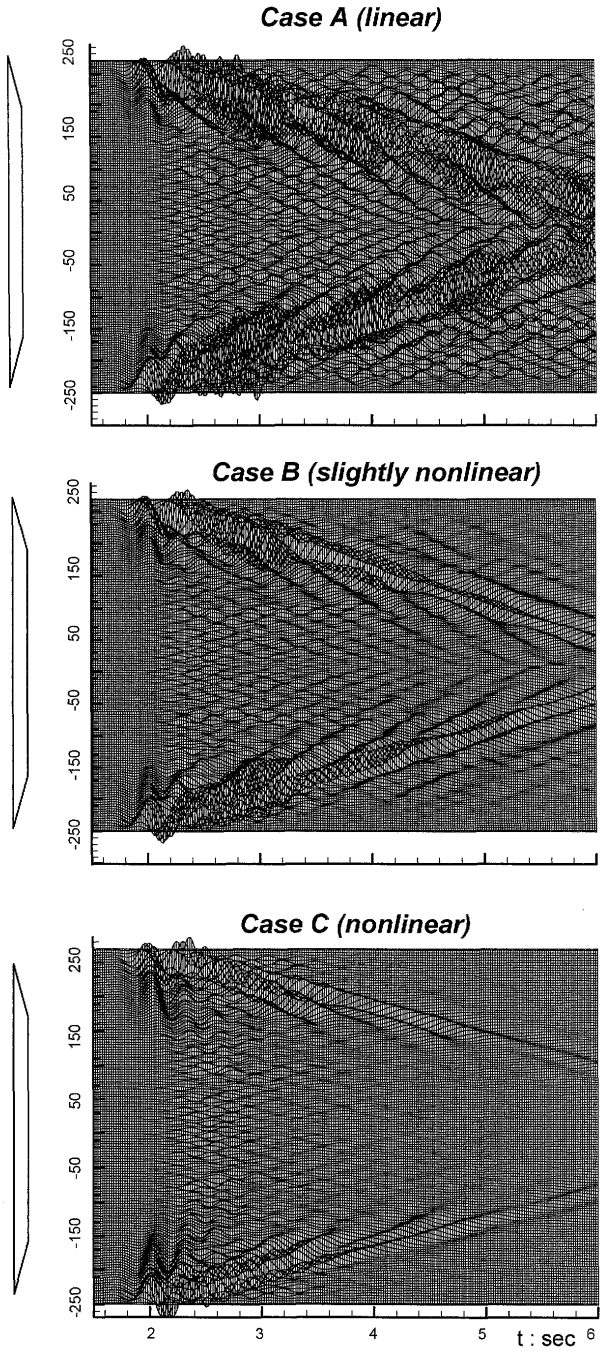

Fig. 23. Wavefields of vertical acceleration calculated along the surface of the valley for the three cases of nonlinearity examined for the high-frequency Ricker pulse ($f_0 = 2$ Hz)

horizontally-polarized particle motion of the incident seismic input (vertically propagating SV waves), the surface response contains additionally a *parasitic* vertical acceleration component which corresponds to the vertical particle motion of the Rayleigh waves. Figs. 19 and 20 show the time histories of the *parasitic* vertical acceleration calculated along the valley surface in the case of the high-frequency and the low-frequency Ricker pulse, respectively. The distributions along the valley surface of the Vertical to Horizontal Amplification Ratio (*VHAR*), defined as the ratio between vertical peak ground surface acceleration and horizontal peak ground base acceleration are given in Figs. 21 and 22, while the corresponding wavefields are shown in Figs. 23 and 24. As expected, this vertical particle motion is substantial at the edges of the valley, but only when soil material behaves linearly. Nonlinearity affects significantly the Rayleigh wave propagation, and therefore diminishes the vertical motion.

CONCLUSIONS AND DISCUSSION

Recorded and analytical evidence reveals that *soil amplification effects* on an alluvial valley cannot be assessed by linear 1-D theory alone. It has been conducted as an attempt to capture the significant 2-D valley effects on the amplitude and the variability of ground shaking of a soft alluvial valley in Japan, the response of which has been recorded during many past earthquakes. Utilising linear 2-D numerical models under SV excitation, we have shown that the observed high amplification was the outcome of the low acceleration levels of the recorded excitations and the high "*plasticity*" *index* of the soft clayey soil layers. Equivalent-linear 2-D analyses, with hypothetically increased intensity of base shaking and/or hypothetically decreased "*plasticity*" *index* of the clayey materials, may both lead to increased nonlinearity of soil response. The significant energy dissipation that takes place in such a case dampens substantially the laterally propagating Rayleigh waves generated at the valley edges,

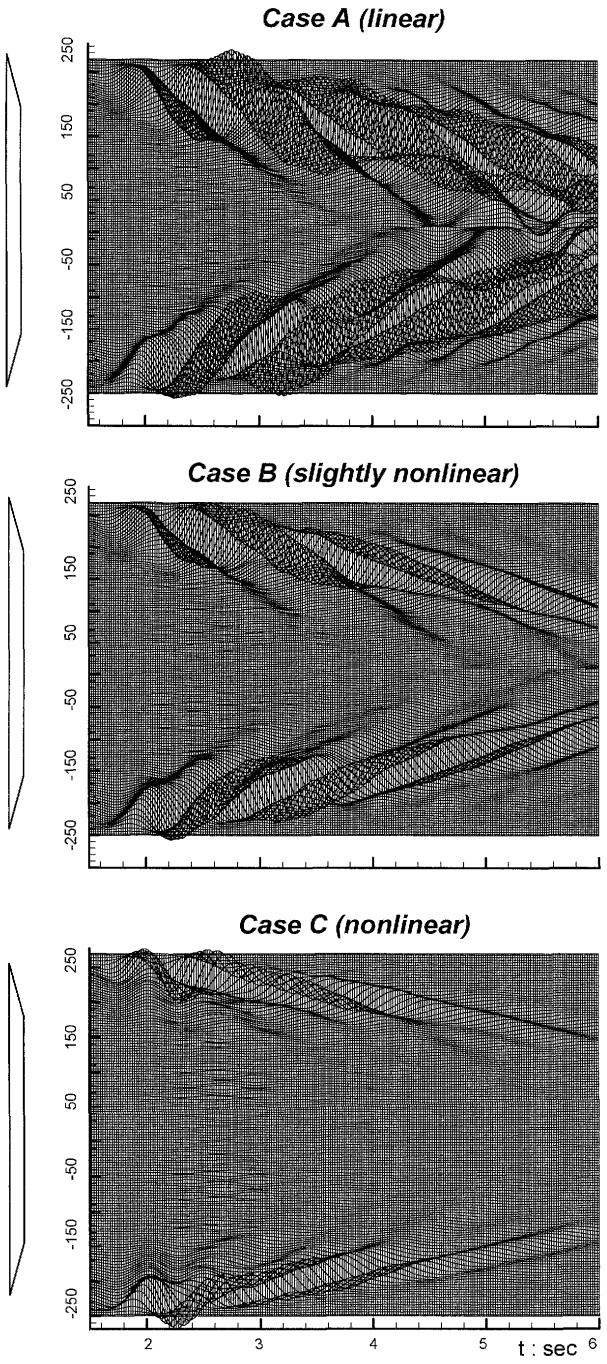

Fig. 24. Wavefields of vertical acceleration calculated along the surface of the valley for the three cases of nonlinearity examined for the low-frequency Ricker pulse ($f_o = 1$ Hz)

while the changing with time soil modulus renders any wave resonance of vertically propagating body waves less important of vertical or inclined body waves from multiple reflections at the interfaces. As a result, the response is dominated by vertical S wave propagation, and thus 1-D soil amplification theory may reproduce the motion satisfactorily (even if somewhat conservatively), provided of course that soil nonlinearity is properly accounted for.

REFERENCES

1) Aki, K. and Larner, K. L. (1970): Surface motion of a layered medium having an irregular interface due to incident plane SH waves, *Journal of Geophysical Research*, **75**, 933–954.
2) Aki, K. (1988): Local site effects on strong ground motion, *Earthquake Engineering and Soil Dynamics II*, ASCE.
3) Aki, K. (1993): Local site effects on weak and strong ground motion, *Tectonophysics*, **218**, 93–111.
4) Bao, H., Bielak, J., Ghattas, O., Kallivokas, L. F., O'Hallaron, D. R., Shewchuk, J. and Xu, J. (1996): Earthquake ground motion modeling on paraller computers, *Proc. ACM/IEEE Supercomputing Conference*, Pittsburgh, USA.
5) Bard, P. Y. and Bouchon, M. A. (1980): The seismic response of sediment filled valleys, Parts I-II, *Bulletin of the Seismological Society of America*, 70.
6) Bard, P. Y. (1997): Local effects on strong ground motion: Basic physical phenomena and estimation methods for microzoning studies, *Notes of the Advanced Study Course SERINA (Seismic Risk: An Integrated Seismological, Geotechnical and Structural Approach)*, Thessaloniki, Greece.
7) Bardet, J. P., Kapuskar, M., Martin, G. R. and Proubet, J. (1992): Site Response of the Marina District of San Francisco during the Loma Prieta Earthquake, *USGS Professional Paper 1551-F*, The Loma Prieta, California, Earthquake of October 17, 1989- Marina District, 85–140.
8) Bielak, J. and Christiano, P. (1984): On the effective seismic input for non-linear soil-structure interaction systems, *Earthquake Engineering and Structural Dynamics*, **12**, 107–119.
9) Bielak, J., Xu, J. and Ghattas, O. (1999): Earthquake ground motion and structural response in alluvial valleys, *Journal of Geotechnical and Geoenvironmental Engineering*, **125**, 413–423.
10) Bielak, J., Hisada, Y., Bao, H., Xu, J. and Ghattas, O. (2000): One- vs two- or three-dimensional effects in sedimentary valleys, *Proc. 12th World Conference on Earthquake Engineering*, New Zealand.
11) Bielak, J., Loukakis, K., Hisada, Y. and Yoshimura, C. (2003): Domain Reduction Method for Three-Dimensional Earthquake Modeling in Localized Regions, Part I: Theory, *Bulletin of the Seismological Society of America*, **93**(2), 817–824.
12) Casadei, F. and Gabellini, E. (1997): Implementation of a 3D coupled spectral-element/finite-element solver for wave propagation and soil-structure interaction simulations, *Technical Report*, Joint Research Center.
13) Chavez-Garcia, F., Raptakis, D., Makra, K. and Pitilakis, K. (2000): Site effects at EURO-SEISTEST-II: Results from 2-D numerical modelling and comparison with observations, *Soil Dynamics & Earthquake Engineering*, **19**(1), 23–39.
14) Faccioli, E., Maggio, F., Paolucci, R. and Quarteroni, A. (1997): 2-D and 3-D elastic wave propagation by a pseudo-spectral domain decomposition method, *Journal of Seismology*, **1**, 237–251.
15) Faccioli, E., Paolucci, R. and Vanini, M. (Editors) (1999): *Three-dimensional Site Effects and Soil-Foundation Interaction in Earthquake and Vibration Risk Evaluation*.
16) Fan, K. (1992): Seismic response of pile foundations evaluated through case histories, *Ph.D Thesis*, S.U.N.Y. at Buffalo.
17) Finn, W. D. L. (1991): Geotechnical engineering aspects of seismic microzonation, *Proc. 4th International Conference on Seismic Zonation*, Stanford, **1**, 199–250.
18) Fukuwa, K, Sato, T., Kawase, H. and Nakai, S. (1985): Simulation of seismic observations in irregular alluvial ground, *Journal of Structural Engineering*, **31**(8), 1–10.
19) Gazetas, G., Fan, K., Tazoh, T. and Shimizu, K. (1993): Seismic response of the pile foundation of Ohba Ohashi bridge, *Proc. 3rd International Conference on Case Histories in Geotechnical Engineering*, St. Louis, 1803–1809.
20) Graves, R. W. (1993): Modeling three-dimensional site response effects in the Marina District Basin, San Francisco, California, *Bulletin of the Seismological Society of America*, **83**, 1042–1063.
21) Graves, R. W. (1996): Simulating seismic wave propagation in 3-D elastic media using staggered grid finite differences, *Bulletin of the Seismological Society of America*, **86**, 1091–1106.
22) Graves, R. W. (1998): Three-dimensional computer simulations of

realistic earthquake ground motions in regions of deep sedimentary basins, *2nd International Symposium on the Effects of Surface Geology on Seismic Motion*, Yokohama, **I**, 103–120.
23) Hibbit, Karlsson, and Sorensen, Inc. (1998): ABAQUS Code.
24) Hisada, Y., Bao, H., Bielak, J., Ghattas, O. and O'Hallaron, D. R. (1998): Simulations of long-period ground motions during the 1995 Hyogoken-Nambu (Kobe) earthquake using 3-D finite element method, *2nd International Symposium on the Effects of Surface Geology on Seismic Motion*, Yokohama, **III**, 1353–1360.
25) Hudson, M., Idriss, I. M. and Beikae, M. (1994): QUAD4M: A computer program to evaluate the seismic response of soil structures using finite element procedures and incorporating a compliant base, *Research Report*, Department of Civil & Environmental Engineering, University of California, Davis.
26) Ishibashi, I. and Zhang, X. (1993): Unified dynamic shear moduli and damping ratios of sand and clay, *Soils and Foundations*, **33**(1), 82–191.
27) Ishihara, K. (1996): *Soil Behaviour in Earthquake Geotechnics*, Oxford University Press.
28) Kawase, H. (1996): The cause of the damage belt in Kobe: "The basin-edge effect", Constructive interference of the direct S-wave with the basin-induced diffracted Rayleigh waves, *Seismological Research Letters*, **67**(5), 25–34.
29) Kokusho, T., Yoshida, Y. and Esashi, Y. (1982): Dynamic properties of soft clay for wide strain range, *Soils and Foundations*, **2**(4), 1–18.
30) Kokusho, T. and Matsumoto, M. (1998): Nonlinearity in site amplification and soil properties during the 1995 Hyogoken-Nambu Earthquake, *Special Issue of Soils and Foundations*, **2**, 1–9.
31) Loukakis, K. (1988): Transient response of shallow layered valleys for inclined SV waves calculated by the finite-element method, *MS Thesis*, Carnegie Mellon University, Pittsburgh, USA.
32) Marsh, J., Larkin, T. J., Haines, A. J. and Benites, R. A. (1995): Comparison of linear and nonlinear seismic responses of two-dimensional alluvial basins, *Bulletin of the Seismological Society of America*, **85**, 874–889.
33) Matsushima, S. and Kawase, H. (1998): 3-D wave propagation analysis in Kobe referring to "The basin-edge effect", *2nd International Symposium on the Effects of Surface Geology on Seismic Motion*, Yokohama, **III**, 1377–1384.
34) NeGe (1992): *Reference Manual*, Department of Civil Engineering, University College of Swansea, UK.
35) Ohtsuki, A., Tazoh, T. and Shimizu, K. (1984): Effect of lateral inhomogeneity on seismic waves and ground strains, *Journal of Structural Mechanics and Earthquake Engineering*, **350**, 291–350.
36) Paolucci, R. (1999): Fundamental vibration frequencies of 2-D geological structures, *Proc. 2nd International Conference on Earthquake Geotechnical Engineering*, Lisbon, **1**, 255–260.
37) Pitarka, A., Irikura, K., Iwata, T. and Sekiguchi H. (1998): Three-dimensional simulation of the near-fault ground motion for the 1995 Hyogoken-Nambu, Japan, earthquake, *Bulletin of the Seismological Society of America*, **88**, 428–440.
38) Psarropoulos, P. N., Gazetas, G. and Tazoh, T. (1999): Seismic response analysis of alluvial valley at bridge site, *2nd International Conference in Earthquake Geotechnical Engineering*, Lisbon, 41–46.
39) Raptakis, D., Chavez-Garcia, F., Makra, K. and Pitilakis, K. (2000): Site efects at EURO-SEISTEST-I: 2-D determination of the valley structure and confrontation of the observations with 1-D analysis, *Soil Dynamics & Earthquake Engineering*, **19**(1), 1–22.
40) Ricker, N. (1960): The form and laws of propagation of seismic wavelets, *Geophysics*, **18**, 40.
41) Sánchez-Sesma, F. J. and Esquivel, J. A. (1979): Ground motion on alluvial valleys under incident plane SH waves, *Bulletin of the Seismological Society of America*, **69**, 1107–1120.
42) Sánchez-Sesma, F. J., Chavez-Garcia, F. and Bravo, M. A. (1988): Seismic response of a class of alluvial valley for incident SH waves, *Bulletin of the Seismological Society of America*, **78**(1), 83–95.
43) Sincraian, M. V. and Oliveira, C. S. (1998): Nonlinear analysis of seismic behaviour of a valley using the finite element method, *Proc. 11th European Conference on Earthquake Engineering*, Paris (in CD Rom).
44) Takemiya, H. (1996): Effects of irregular soil profile on strong ground motion, *The 1995 Hyogoken-Nanbu Earthquake*, Japan Society of Civil Engineers, 15–26.
45) Tazoh, T., Dewa, K., Shimizu, K. and Shimada, M. (1984): Observations of earthquake response behavior of foundation piles for road bridge, *Proc. 8th World Conference on Earthquake Engineering*, **3**, 577–584.
46) Tazoh, T., Shimizu, K. and Wakahara (1988): Seismic observations and analysis of grouped piles, *Shimizu Technical Research Bulletin*, **7**, 17–32.
47) Trifunac, M. D. (1971): Surface motion of a semi-cylindrical alluvial valley for incident plane SH waves, *Bulletin of the Seismological Society of America*, **61**, 1755–1770.
48) Vucetic, M. and Dobry, R. (1991): Effect of soil plasticity on cyclic response, *Journal of Geotechnical Engineering*, ASCE, **117**, 89–107.
49) Xu, J., Bielak, J., Ghattas, O. and Wang, J. (2002): Three-dimensioanl seismic ground motion modeling in inelastic basins, *Physics of the Earth and Planetary Interiors*, **137**, 81–95.
50) Yegian, M. K., Ghahraman, V. G. and Gazetas, G. (1994): Seismological, soil and valley effects in Kirovakan, 1988 Armenia earthquake, *Journal of Geotechnical Engineering*, ASCE, **120**(2), 349–365.
51) Yoshimura, C., Bielak, J., Hisada, Y. and Fernandez, A. (2003): Domain reduction method for three-dimensional earthquake modeling in localized regions, Part II: verification and applications, *Bulletin of the Seismological Society of America*, **93**(2), 817–824.
52) Zhang, B. and Papageorgiou, A. S. (1996): Simulation of the response of the Marina District Basin, San Francisco, CA., to the 1989 Loma Prieta earthquake, *Bulletin of the Seismological Society of America*, **86**(5), 1382–140.